

Infrared Reflection Absorption Study of Carbon Monoxide Adsorbed on Submonolayer Fe-Covered Cu(100), (110), and (111) Bimetallic Surfaces

Toshimasa Wadayama,* Kazumi Kubo, Terumasa Yamashita, Tadao Tanabe, and Aritada Hatta

Department of Materials Science, Graduate School of Engineering, Tohoku University, Sendai 980-8579, Japan

Received: May 30, 2002; In Final Form: December 12, 2002

Carbon monoxide (CO) adsorption at 90 K on Cu(100), (110), and (111) covered with submonolayer Fe at room temperature has been investigated using infrared reflection absorption spectroscopy (IRRAS). Saturated adsorption of CO on the 0.3-monolayer (ML)-thick Fe/Cu(111) bimetallic surface yields two C–O stretch bands at 2075 and 2015 cm^{-1} due to adsorption on the uncovered Cu and on deposited Fe, respectively. The former band agrees in frequency with the C–O stretch band on the clean Cu(111) surface, indicating that the deposited Fe does not affect the Cu surface. In contrast, on the 0.3-ML Fe/Cu(100) surface, an additional C–O stretch band emerges at 2104 cm^{-1} on the high-frequency side of the band (2090 cm^{-1}) due to CO adsorbed on the uncovered Cu surface. This band arises from CO bound to Cu atoms formed by intermixing of the deposited Fe and substrate Cu atoms. Even more intense Fe–Cu intermixing occurs on the 0.3-ML Fe/Cu(110) surface; for saturated adsorption, the corresponding band is observed at 2108 cm^{-1} , and its relative intensity to the C–O band on the uncovered Cu surface is much stronger than on the 0.3-ML Fe/Cu(100) surface. This severe intermixing at the Cu(110) substrate surface is explained in terms of a high surface energy and the specific surface lattice structure.

1. Introduction

Surface reactivity or selectivity has been the subject of many investigations in the field of catalysis. There is sufficient evidence that bimetallic surfaces have new catalytic properties that are different from those of the component elements; this feature has been explained in terms of “ensemble” and “ligand” effects.¹ Molecular-beam epitaxy (MBE) and ultrahigh vacuum (UHV) techniques allow us to create high-quality bimetallic systems. Actually, such systems are good candidates for heterogeneous catalysts² and microelectronics materials.³ An interesting example of the man-made bimetallic system is Fe–Cu.^{4–12} The bulk Fe crystal has a body-centered cubic (bcc) structure at temperatures below 1190 K. However, when deposited on single-crystal Cu substrates, face-centered cubic (fcc) metastable Fe grows even at room temperature because of a very low lattice mismatch between Cu (3.61 Å) and Fe (3.59 Å). Since ultrathin films of fcc-Fe grown on Cu exhibit unique magnetic properties, a number of studies have been made in view of the applicability of this system. The combination of the transition metals Cu and Fe is also of catalytic interest because of their different chemical properties; Cu is useful for oxidation reactions whereas Fe plays an important role in the ammonia and Fischer–Tropsch syntheses.

Among the various types of spectroscopic techniques used to investigate metal surfaces, infrared reflection absorption spectroscopy (IRRAS) has gained wide recognition for its ability to detect and characterize surface-adsorbed species with high sensitivity and resolution. It has been demonstrated^{13–19} that CO can be used to probe surface lattice structures as well as the electronic properties of metal surfaces. However, only a very limited amount of work has been reported to date on the surface

chemistry of ultrathin fcc-Fe films grown on Cu single-crystal surfaces.^{20–23} Thus, we have previously investigated CO adsorption at 90 K on molecular-beam-deposited fcc-Fe thin films on Cu(100) and Cu(111) using IRRAS.^{24–26} Our experimental evidence²⁵ shows that for a two-monolayer (ML) coverage of Fe on Cu(100) a specific band appears at 2104 cm^{-1} , which is much higher than the C–O stretching frequency of CO adsorbed on the clean Cu(100) surface. However, this band could not be observed for larger Fe coverages on Cu(100).^{24,25} In contrast, such a high-frequency band was not observed at any coverages of Fe on Cu(111).²⁶ Thus, the high-frequency band was assigned to the C–O stretch of CO bound to Cu intermixed with Fe.²⁵ In view of these results, it seemed that a further extension of our previous work to the system fcc-Fe/Cu(110) is useful for a better understanding of the intermixing phenomenon. Such an understanding may also provide us deeper insight into the catalytic properties of Fe–Cu bimetallic surfaces. These indeed are our motivations for the present work.

In the present paper, we investigate CO adsorption at 90 K on submonolayer Fe-deposited Cu(100), (111), and (110) surfaces using IRRAS. All of the Cu surfaces covered with 1.0-monolayer (ML)-thick Fe exhibited two C–O stretch bands due to CO adsorbed on the Fe and the uncovered Cu surface, revealing the formation of Fe islands. However, both 0.3-ML Fe/Cu(100) and 0.3-ML Fe/Cu(110) bimetallic surfaces showed an additional band due to CO bound to Cu atoms intermixed with Fe, the intensity of which is stronger on the latter than on the former surface. This can be explained by the difference in surface energy and/or in surface atomic structure between Cu(100) and Cu(110). In agreement with this view, no C–O stretch band due to Fe–Cu intermixing was observed on the 0.3-ML Fe/Cu(111) surface. These results demonstrate that IRRAS investigations of CO adsorption provide useful information not only on the adsorption/desorption behavior of CO on the Fe/

* To whom correspondence should be addressed. E-mail: wadayamt@material.tohoku.ac.jp. Phone: +81-22-217-7319. Fax: +81-22-217-7374.

TABLE 1: Vibrational C–O Stretch Frequency Bands for CO Adsorbed on Fe, Cu, and Fe/Cu Bimetallic Surfaces

substrate	lattice	ν CO frequency (cm^{-1})
Fe(100) (bulk) ^d	bcc	1900–2055 (on top), 1180–1245 (lying down)
Fe(111) (bulk) ^b	bcc	1940–2015 (on top), 1735–1860 (shallow hollow), 1325–1575 (deep hollow)
Fe(110) (bulk) ^c	bcc	1890–1985 (on top), 1180–1245 (lying down)
poly Fe (film) ^d	bcc	2055 (on top)
Fe(100) (epitaxial) ^d	fcc	1920–2048 (bridge and on top)
Fe(111) (epitaxial) ^e	fcc	1930–2000 (bridge and on top)
Cu(100) (bulk) ^f	fcc	2079–2088 (on top)
Cu(111) (bulk) ^g	fcc	2070–2080 (on top)
Cu(110) (bulk) ^h	fcc	2088–2104 (on top)
Fe/Cu(100) ⁱ		1940–1950 (Fe: bridge), 2000–2010 (Fe: on top), 2090 (Cu: uncovered), 2104–2110 (Cu: intermixed)
Fe/Cu(111) ⁱ		1975–2015 (Fe: bridge and on top), 2073–2078 (Cu: uncovered)
Fe/Cu(110) ⁱ		1990–2025 (Fe: bridge and on top), 2091 (Cu: uncovered), 2103–2118 (Cu: intermixed)

^a Reference 31. ^b Reference 32. ^c Reference 33. ^d Reference 34. ^e Reference 26. ^f Reference 29. ^g References 27 and 28. ^h Reference 30. ⁱ Present work.

Cu bimetallic surface but also on the aggregation and stability of deposited Fe layers on Cu.

2. Experimental Section

Details of the experimental equipment and methods used in the present work have been reported elsewhere.^{24–26} Briefly, Cu(100), (110), and (111) crystals of less than 1° miscut were electrochemically polished and used as substrates for Fe deposition. Each surface was cleaned by repeated Ar⁺ sputtering and annealing under UHV conditions. After the cleaning procedures, surface cleanliness and crystallographic order were verified with reflection high-energy electron diffraction (RHEED), low-energy electron diffraction (LEED), and Auger electron spectroscopy (AES). Additionally, the Cu surfaces were allowed to adsorb CO before Fe deposition, and thereby we confirmed that these surfaces gave a sharp C–O stretch band, as reported in the literature.^{27–30} Fe of 99.999% purity was deposited using a Knudsen cell onto the Cu substrate surfaces held at room temperature. Fe film thicknesses in ML units on all of the Cu surfaces were estimated on the basis of deposition time and the number of regular oscillations in the RHEED intensity observed during the fcc-Fe/Cu(100) epitaxial growth.^{24,25} The deposition rate of Fe was approximately 0.3 ML/min. Each of the samples thus prepared was immediately cooled to 90 K and then exposed to CO at a pressure of approximately 7×10^{-10} Torr. The pressure of the chamber before CO introduction was less than 1×10^{-10} Torr. The IRRAS spectra were recorded at 2-cm⁻¹ resolution as the average of 300 scans using an FT-IR spectrometer (Mattson RS-2) equipped with a liquid-N₂-cooled HgCdTe detector. Each of the spectra was compared to the spectrum obtained before CO exposure.

3. Results and Discussion

3.1. CO Adsorption on Submonolayer Fe/Cu(100) Bimetallic Surfaces. The RHEED image obtained before Fe deposition showed sharp streaks with some Kikuchi bands that were expected only for a clean Cu(100) surface. In the Fe thickness range (less than 1.0 ML) investigated in the present work, essentially the same RHEED image as that from clean Cu(100) was observed, suggesting Fe deposition with an fcc-(100) geometry on the Cu surface.

The C–O stretch frequencies for different adsorption sites of Fe, Cu, and Fe/Cu bimetallic surfaces, investigated earlier^{26–34} and in the present work, are summarized in Table 1, showing the differences and similarities between adsorption on the submonolayer Fe/Cu surfaces compared with that of the bulk Fe and Cu surfaces.

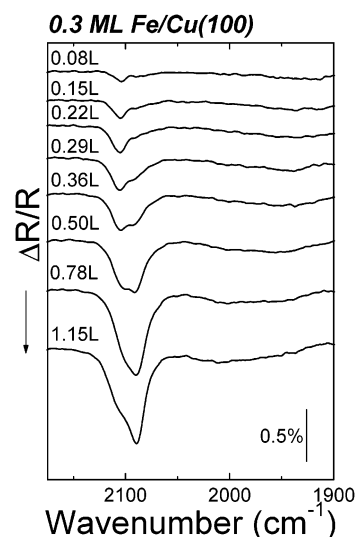


Figure 1. IRRAS spectra of CO adsorbed on 0.3-ML Fe/Cu(100) at 90 K as a function of increasing CO exposure.

Figure 1 shows the IRRAS spectra of adsorbed CO molecules on 0.3-ML Fe/Cu(100) at 90 K as a function of increasing CO exposure. In the early stages of exposure (0.29 L; 1 L = 10^{-6} Torr s), three bands appear at 2104, 2090 (shoulder), and 1940 cm⁻¹. The 1940-cm⁻¹ band shifts to 1950 cm⁻¹ at 0.50-L exposure. At this exposure, a new band appears at 2000 cm⁻¹, which shifts to 2010 cm⁻¹ at saturation coverage (1.15 L). However, the high-frequency bands (2104 and 2090 cm⁻¹) increase in intensity with increasing exposure, but they shift very little even though the exposure is increased up to saturation.

Our previous investigations of the adsorption behavior of CO on fcc-Fe films epitaxially grown on Cu(100)^{24,25} showed that the bands due to CO adsorption at the bridge and on-top sites of the Fe surfaces were located in the 1920–2000 and 2000–2040 cm⁻¹ regions, respectively (Table 1). Therefore, the two bands observed at 1940–1950 and 2000–2010 cm⁻¹ in Figure 1 can be assigned to CO adsorbed at the bridge and on-top sites of the deposited Fe surface, respectively. In view of the small Fe coverage, the low intensities of these bands even at the saturation coverage (1.15 L) can be explained by the formation of small Fe domains on the Cu(100) surface. The blue shifts of these bands with increasing CO exposure suggest an increased dipole–dipole coupling among adsorbed CO molecules and a decreased electron back-donation from the metal d bands to the unoccupied CO 2 π^* orbital, as is commonly argued for CO adsorption on metal surfaces.^{17–19}

It has been reported^{27,28,35,36} that CO adsorption on clean Cu(100) gives a C–O stretch band at 2079–2088 cm⁻¹ and that

its desorption occurs at 200 K. We therefore ascribe the band at 2090 cm^{-1} to CO molecules on the on-top sites of the uncovered Cu(100) surface. The position of the 2104-cm^{-1} band, however, is about 15 cm^{-1} higher than the C—O stretch band on clean Cu(100); furthermore, as will be shown later, it disappears at 216 K. This temperature is 15 K higher than the desorption temperature of CO on the clean surface. It has been shown on the basis of scanning tunneling microscopy (STM) that at the early stages of deposition Fe grows on Cu(100) with 3D island structures.^{8,37–41} Moreover, Chambliss et al.^{42–45} deduced from STM measurements that intermixing with Fe occurs on Cu(100) upon Fe deposition even at room temperature. In that case, the initial process of Fe epitaxy on the Cu surface is an exchange of incoming Fe atoms with surface Cu atoms, and the first layer consists of the Cu atoms displaced by the Fe—Cu exchange.

It is also likely that electronic configurations of such Cu clusters or Cu atoms should differ from those of Cu(100). Actually, Moskovits and Hulse⁴⁶ reported IR absorption frequencies of CO on Cu clusters using a matrix isolation method and showed that the C—O stretch frequency shifts from 2128 to 2103 cm^{-1} with an increasing number of Cu atoms from 2 to 4. Furthermore, Hoffmann and Paul^{15,16} investigated CO adsorption on a Cu/Ru(001) bimetallic surface with IRRAS, which showed that the C—O stretch frequencies of adsorbed CO on Cu clusters of 1–4 atoms, 2D Cu aggregates, and 3D Cu aggregates were $2123\text{--}2138\text{ cm}^{-1}$, $2110\text{--}2120\text{ cm}^{-1}$, and 2098 cm^{-1} , respectively. These facts make it plausible that the band observed at 2104 cm^{-1} in Figure 1 can be assigned to adsorbed CO on Cu atoms formed through intermixing of the deposited Fe and the substrate Cu atoms. However, it appears that the number of Cu atoms in the top surface layer pertaining to the adsorption is not directly determined from the band intensity and the position (i.e., 2104 cm^{-1}) on the basis of the IR data for the isolated Cu clusters⁴⁶ described above since chemical modifications of the Cu atoms by intermixing with the Fe atoms may in fact be important.

As is evident from Figure 1, the band at 2104 cm^{-1} steadily increases in intensity with increasing CO exposure whereas the 2090-cm^{-1} band increases slowly at first and then more rapidly until saturation at 1.15 L. The results clearly show that CO molecules are preferentially bound to the Fe-intermixed Cu atoms and subsequently adsorbed on the uncovered Cu(100) surface. This preferential adsorption may be explained in terms of the stability of adsorbed CO molecules; it is higher for adsorption onto the Fe-intermixed Cu atoms than onto the uncovered Cu surface. It is likely that the Cu atoms isolated in the top Fe surface layer have localized sp states,⁴⁷ which may promote charge transfer from the 5σ molecular orbital of CO to the Cu atoms, thereby stabilizing the adsorption.

Subsequently, we examined the thermal desorption for CO adsorbed to saturation at 90 K on the 0.3-ML Fe/Cu(100) surface. The IRRAS spectra obtained during the elevation of the substrate temperature up to 238 K are shown in Figure 2. No spectral measurements at higher temperatures were made to avoid possible intermixing between the deposited Fe and the substrate Cu. It is seen from Figure 2 that whereas the band at 2088 cm^{-1} completely disappears at 200 K the 2104-cm^{-1} band due to CO bound to the Fe-intermixed Cu atoms disappears at 238 K. It follows then that the CO desorption temperature from these sites is at least 15 K higher than that on clean Cu(100).³² One may notice a band at 1945 cm^{-1} , which increases very little in intensity as the substrate temperature is increased from 170 to 188 K but rather rapidly increases when the temperature

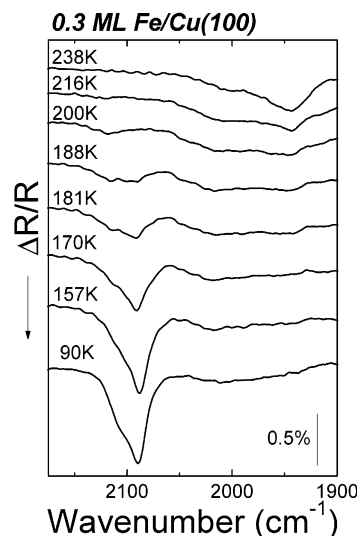


Figure 2. IRRAS spectral changes of CO adsorbed on 0.3-ML Fe/Cu(100) during rising substrate temperature.

is raised from 216 to 238 K. In view of the frequency, we attribute this band to CO adsorbed at the bridge sites of the deposited Fe film.^{24,25}

Figure 2 also shows that as the temperature is increased from 216 to 238 K the band (ca. 2100 cm^{-1}) due to on-top bonded CO molecules on the Fe surface decreases in intensity and shifts to lower frequency whereas the 1945-cm^{-1} band rapidly increases, as mentioned above. This suggests that part of the on-top bound CO molecules migrated to the bridge sites of the Fe surface. In other words, the bridge sites of the Fe surface are more favorable adsorption sites for CO than the on-top sites.⁴⁸ The spectra shown in Figure 2 reveal that desorption of CO first occurs from the uncovered Cu(100) surface, then from the Fe-intermixed Cu atoms, and finally from the on-top sites of the deposited Fe film. This desorption sequence corresponds well to the exposure-dependent spectra shown in Figure 1, where we can see preferential CO adsorption on the Fe-intermixed Cu atoms. A thermal migration of CO from the uncovered Cu to Fe sites was also observed on Fe/Cu(111) and Fe/Cu(110) bimetallic surfaces.

IRRAS measurements were also carried out for CO adsorbed to saturation on Cu(100) covered with different submonolayer coverages of Fe ranging from 0.3 to 1.0 ML. The results are shown in Figure 3, together with the spectrum of adsorbed CO on the clean Cu(100) surface before Fe deposition. There can be seen three C—O stretch bands arising from adsorption on the uncovered Cu surface, Fe-intermixed Cu atoms, and the deposited Fe. It is clear that the band near 2090 cm^{-1} due to CO on the uncovered Cu(100) surface decreases in intensity and shifts to higher frequency as the Fe coverage increases from 0.5 to 1.0 ML. CO adsorption on the deposited Fe gives a broad band peaking at 2100 cm^{-1} for 0.3 ML Fe coverage, and this band abruptly increases in intensity and shifts to higher frequency as the coverage increases to 0.7 ML. Moreover, the C—O stretch band (shoulder) associated with the Fe-intermixed Cu atoms (2104 cm^{-1} for 0.3 ML) shifts to higher frequency (2110 cm^{-1}) for 1.0 ML coverage. These spectral changes suggest some changes in the aggregation or dispersion of Fe on the Cu substrate and in the manner of intermixing with the substrate Cu atoms as well, each of which should vary with Fe coverage.

Indeed, the LEED image of a CO adlayer on the 0.1-ML-thick Fe/Cu(100) surface gave a clear $c(2 \times 2)$ structure that is

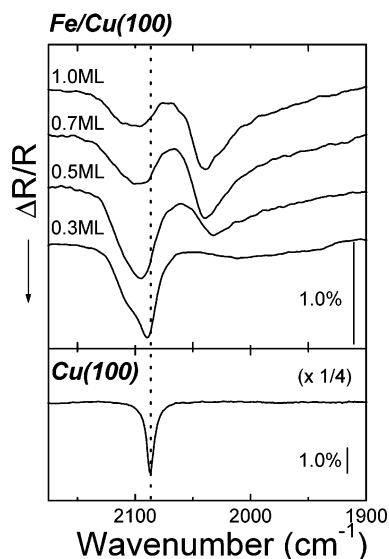


Figure 3. IRRAS spectra of CO for saturated adsorption at 90 K on Fe/Cu(100) as a function of Fe coverage.

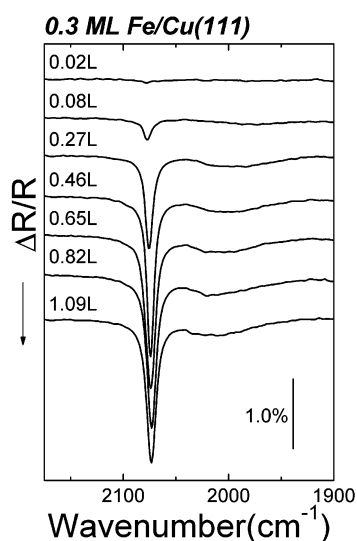


Figure 4. IRRAS spectra of CO adsorbed on 0.3-ML Fe/Cu(111) at 90 K as a function of increasing CO exposure.

typical for adsorbed CO on Cu(100),⁴⁹ but for the CO adlayer on the 0.5-ML Fe film, the contrast of the half-order spots decreased significantly. On the 1.0 ML Fe/Cu(100) surface, only the primitive (1×1) spots were seen in the LEED image, suggesting that the adsorbed CO molecules on the surface form no long-range-ordered overlayer structure. The decrease in contrast of the $c(2 \times 2)$ pattern corresponds well to the decrease in intensity of the 2090- cm^{-1} band due to CO adsorption on the uncovered Cu (100) surface (Figure 3).

3.2. CO Adsorption on Submonolayer Fe/Cu(111) Bimetallic Surfaces. Before Fe deposition on the Cu(111) surface, sharp streaks with some Kikuchi bands as expected for clean Cu(111) were observed in the RHEED image. Essentially the same image was obtained for the submonolayer Fe coverage. Although the streaks observed during Fe deposition showed no regular intensity oscillations, the observed image suggested the epitaxial growth of Fe on the Cu surface.

The IRRAS spectra of CO adsorbed on the 0.3-ML Fe/Cu(111) surface at 90 K are shown as a function of CO admission in Figure 4. Two bands appear at 2078 cm^{-1} and at around 1975 cm^{-1} for a small CO admission of 0.08 L. With increasing

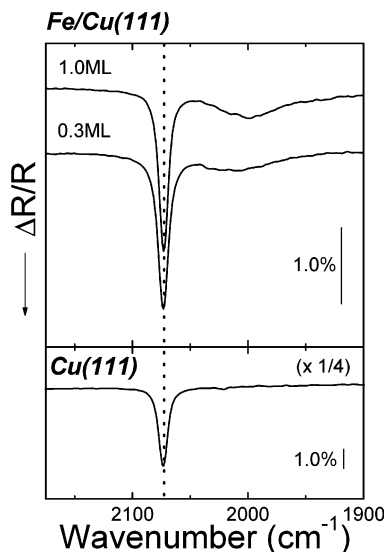


Figure 5. IRRAS spectra of CO for saturated adsorption on Fe/Cu(111) at 90 K.

CO exposure, the former band increases in intensity and shifts to 2073 cm^{-1} at 1.09 L. The latter band increases in intensity, accompanied by a blue shift with increasing exposure up to 0.27 L, above which it is rather constant in intensity and in position (ca. 2015 cm^{-1} at 1.09 L). The IRRAS investigations of CO adsorbed on clean Cu(111) reported by Horn and Prichard³⁵ showed that the on-top-site adsorption yields a single band at 2073 cm^{-1} . This fact allows an assignment of the 2073- cm^{-1} band to the on-top adsorption on the uncovered Cu(111) surface. Our previous IRRAS investigations of CO adsorption on the epitaxial fcc-Fe/Cu(111) surfaces at 90 K²⁶ showed that adsorbed CO on the fcc-Fe(111) surface exhibits a single band in the 1930–2000 cm^{-1} region (Table 1). Furthermore, the band position for CO adsorbed at saturation on 0.3-ML Fe shifts to lower frequency with increasing Fe coverage from 0.3 to 1.0 ML, as shown in Figure 5. Thus, the low-frequency band observed in Figure 4 is ascribable to CO adsorbed on the on-top sites of the deposited Fe surface because of its high frequency.

The IRRAS spectra for saturation adsorption of CO on clean and Fe-deposited Cu(111) surfaces are depicted in Figure 5, where two absorption bands are observed at 2073 and 2015–2000 cm^{-1} . As the Fe coverage is increased from 0.3 to 1.0 ML, the low-frequency band at 2015 cm^{-1} increases in intensity, accompanied by a red shift to 2000 cm^{-1} , whereas the high-frequency band at 2073 cm^{-1} remains almost unchanged in intensity and in position. Although the red shift of the low-frequency band is not yet understood, its intensity increase with increasing Fe coverage may be taken as a result of growth domains of Fe on the Cu substrate. Considering the small Fe coverage dependence of the 2073- cm^{-1} band, the formation of higher Fe islands than in the case of 0.3-ML Fe/Cu(111) is suggested. In fact, our previous RHEED observation²⁶ of the Fe epitaxy on Cu(111) showed no regular oscillation of the intensity of the RHEED reflexes, indicating no layer-by-layer growth. In either case of 0.3- or 1.0-ML deposition, preferential island formation at the edges of the Cu crystal is possible, together with a concomitant formation of Cu holes due to the relaxation of tensile stress.⁵⁰

It is significant that whereas in the Fe/Cu(100) system the stretch band of CO bound to Fe-intermixed Cu atoms was observed, no corresponding band is observed in the Fe/Cu(111) system. Furthermore, the 2073- cm^{-1} band observed after 1.0-

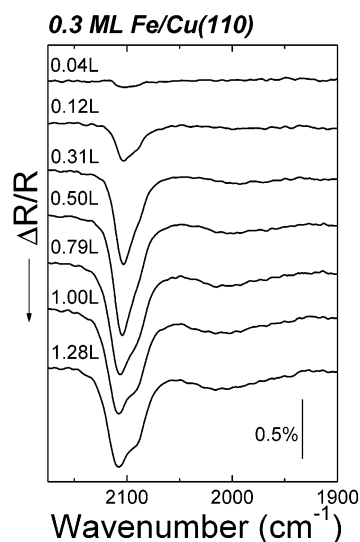


Figure 6. IRRAS spectra of CO adsorbed on 0.3-ML Fe/Cu(110) at 90 K as a function of increasing CO exposure.

ML Fe deposition is very narrow, and its half-width (9 cm^{-1}) is almost identical to that observed on the clean Cu(111) surface, as shown in Figure 5. These features appear to indicate that the 1.0-ML Fe deposition has no serious influence on the Cu(111) surface. The same holds true for the 0.3-ML deposition; in this case, the 2073-cm^{-1} band is only a little broader but at the same position as the C—O stretch band observed for the clean Cu(111) surface. Moreover, if the integrated CO band intensity on the uncovered Cu(111) surface is taken into account, then the total area of the uncovered Cu surface at 0.3-ML coverage is nearly the same as that at 1.0-ML coverage. Thus, the dependence of Fe coverage on the low-frequency band shown in Figure 5 must be accounted for by differences in both the dimensions and distribution of Fe islands between 0.3- and 1.0-ML depositions on the Cu substrate. The LEED image obtained for the CO adlayer on the 0.3-ML Fe-deposited Cu(111) surface showed a $(\sqrt{3} \times \sqrt{3})\text{-R}30^\circ$ structure, which is typically observed for clean Cu(111).⁵¹ This demonstrates the presence of sufficient free Cu(111) surface area.

3.3. CO Adsorption on Submonolayer Fe/Cu(110) Bimetallic Surfaces. The RHEED image of the Cu(110) surface gave rise to a bright streak pattern with derived atomic spacings being consistent with those expected for Cu(110). When Fe deposition proceeded, though the distance between streaks remained unchanged within the submonolayer Fe coverage range, the contrast of the image had already abruptly decreased at 0.1 ML, suggesting that the deposited Fe film was atomically dispersed in comparison to those on the Cu(100) and Cu(111) surfaces.

Figure 6 shows the IRRAS spectra of CO adsorbed on a 0.3-ML Fe/Cu(110) surface at 90 K as a function of increasing CO exposure. For CO admission at 0.31 L, three C—O stretch bands are observed at 1990, 2091(shoulder), and 2103 cm^{-1} . The 1990-cm^{-1} band increases in intensity with increasing CO admission accompanied by a blue shift and is finally positioned at 2015 cm^{-1} at saturation coverage (1.28 L). Taking into account our published IR results for CO adsorption on fcc-Fe surfaces^{24–26} (Table 1), the lowest-frequency band in the region of 2000 cm^{-1} is ascribable to CO adsorbed on the on-top sites of the deposited Fe film. In this case, we have to consider the dipole–dipole coupling between adsorbed CO molecules on the deposited Fe, which increases with increasing CO admission and results in the blue shift. The position of the shoulder band (2091 cm^{-1})

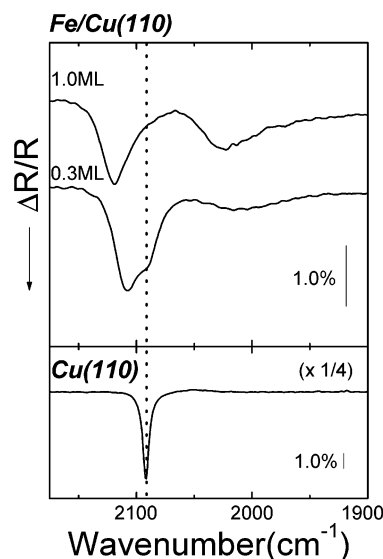


Figure 7. IRRAS spectra of CO for saturated adsorption at 90 K on Fe/Cu(110) as a function of Fe coverage.

is close to the frequency of adsorbed CO on the on-top sites of clean Cu(110)³⁰ and can be attributed to adsorption on the uncovered Cu(110) surface. Since the most prominent band at 2103 cm^{-1} is almost the same in position as the band observed in the 0.3-ML Fe/Cu(100) system, it can be attributed to CO bound to Fe-intermixed Cu atoms. This band as well as the band due to adsorption on the uncovered Cu(110) surface remains almost unchanged in intensity for exposures above 0.79 L.

As the admission is increased, the band relevant to the intermixed Cu atoms is saturated in intensity at 0.5 L and shifts to 2106 cm^{-1} at 1.28 L. Similarly, the band due to CO on the uncovered Cu surface is saturated in intensity at 0.5 L, although no shift occurs as the exposure is increased up to 1.28 L. According to Horn et al.,³⁰ a transition occurs from a (2×1) to a (1.3×2) structure for CO adsorption on Cu(110) during CO admission increases. Therefore, it seems plausible that the above adsorption behavior during CO admission may be related to a change in the adsorbed CO structure on the uncovered Cu(110) surface. Unfortunately, since in our case the 0.3-ML Fe/Cu(110) surface before CO admission gave streaky spots in the LEED image, no further attempt was made to distinguish between the detailed CO adlayer structures.

The IRRAS spectra of CO adsorbed to saturation on Fe/Cu(110) are shown as a function of Fe coverage in Figure 7. At 0.3-ML coverage, three bands (2106 , 2091 , and 2015 cm^{-1}) can be seen in the spectrum. The band at 2091 cm^{-1} (shoulder) is obviously due to adsorption on the uncovered Cu surface whereas the 2015-cm^{-1} band is due to adsorption on the on-top sites of the deposited Fe surface. This band shifts to 2025 cm^{-1} with an increase in intensity at 1.0 ML, a feature similar to that in the case of Fe/Cu(100) (Figure 3). Probably the most significant fact in Figure 7 is that the shoulder at 2091 cm^{-1} for 0.3 ML disappears almost completely at 1.0 ML, for which the band at 2106 cm^{-1} due to CO bound to the Fe-intermixed Cu atoms shifts to 2118 cm^{-1} with seemingly little change in intensity. The disappearance of the 2091-cm^{-1} band for the Fe coverage at 1.0 ML results from more intense intermixing of the deposited Fe and substrate Cu atoms. The intermixing in the present Fe/Cu(110) system is substantially stronger than in the Fe/Cu(100) system, as evidenced from a comparison of the intensity for the highest-frequency band between Figures 7 and 3; at any coverage, the band is much stronger in the former than in the latter.

3.4. Differences in Fe Aggregation on Cu(100), (111), and (110) Surfaces. It has already been shown that for 1.0-ML Fe deposition on Cu(100), (111), and (110) substrates the C—O stretch band at a saturation coverage on the Fe surfaces appears in the region of 2040–2000 cm^{-1} . However, the band due to saturated CO adsorption at the Fe-intermixed Cu atoms is located at 2106 (0.3 ML)–2118 cm^{-1} (1.0 ML) for Fe/Cu(110) and at 2104 (0.3 ML)–2110 cm^{-1} (1.0 ML) for Fe/Cu(100). However, no corresponding band was observed in the Fe/Cu-(111) system. In addition, the relative intensity of the band due to CO bound to the intermixed Cu atoms with respect to that of the band on the uncovered Cu surface is stronger for Fe/Cu-(110) than for Fe/Cu(100). This difference could be caused by the difference in surface energy and/or in surface atomic structure. According to the literature,⁵² the surface energies of Cu(111), (100), and (110) are 3.373, 3.789, and 5.590 J/m², respectively. Additionally, the topmost Cu atoms of (110) in particular form a trench structure. This specific structure as well as the higher surface energy for (110) compared to that of (100) would result in more intense Fe—Cu intermixing. We thus conclude that severe Fe—Cu intermixing gives rise to a strong C—O stretch band at high frequencies (above 2100 cm^{-1}) in addition to a band in the region of 2040–2025 cm^{-1} due to adsorption on the Fe islands.

As mentioned above, little intermixing takes place on the Cu-(111) surface; Fe deposition at 1.0 ML on this surface yields a band at 2000 cm^{-1} due to CO bonding to the deposited Fe that has an fcc lattice structure.²⁶ However, the 1.0-ML Fe film deposited on the Cu(100) surface has no complete layer-by-layer structure.²⁵ In fact, STM observations for submonolayer Fe epitaxy on Cu(100)⁴³ are summarized as follows: The epitaxial surface consists of first-layer islands with a broad distribution of sizes at 0.23 ML of Fe whereas Fe island growth is distributed between the first and second layers and still 15% of the Cu substrate surface is uncovered. The Fe structure on the Cu(110) surface is more in doubt. We cannot rule out the possibility that the deposited Fe is affected by intermixing with Cu either on the (110) surface or on the (100) surface.

4. Summary

In the present study, we have studied the CO adsorption behavior on Cu(100), (111), and (110) surfaces covered with submonolayers of Fe using IRRAS. Even for the deposition of 1.0 ML on these surfaces, the C—O stretch bands on both the deposited Fe and free Cu appear in the IRRAS spectra, revealing the formation of Fe islands. In the Fe/Cu(100) system, an additional C—O stretch band ascribable to CO bonding to Fe-intermixed Cu atoms appears. This band is located on the high-frequency side of the stretch band because of adsorption on the uncovered Cu(100) surface. We conclude that more-intense intermixing occurs for the Fe/Cu(110) system by reference to the intensity of the high-frequency band versus the CO band intensity on the uncovered Cu surface. In contrast, no corresponding band appears on Fe/Cu(111). Such differences in the extent of intermixing can be explained in terms of the surface energy and/or the specific surface atomic structure of the Cu substrate. Thus, the present work provides vibrational spectroscopic evidence for the intermixing of Fe and Cu atoms at room temperature when submonolayer Fe is deposited on Cu(110) and (100). This intermixing does not occur on Cu(111).

References and Notes

- (1) Rodriguez, J. A.; Goodman, D. W. *J. Phys. Chem.* **1991**, 95, 4196.
- (2) Campbell, C. T. *Annu. Rev. Phys. Chem.* **1990**, 41, 775.

- (3) Baibich, M. N.; Broto, J. M.; Fert, A.; Nguyen Van Dau, F.; Petroff, F.; Etienne, P.; Creuset, G.; Friedrich, A.; Chazelas, J. *Phys. Rev. Lett.* **1988**, 62, 2472.
- (4) Kief, M. T.; Egelhoff, W. F., Jr. *Phys. Rev. B* **1993**, 47, 10785.
- (5) Wuttig, M.; Feldmann, B.; Flores, T. *Surf. Sci.* **1995**, 331–333, 659.
- (6) Egelhoff, Jr., W. F. *Surf. Sci.* **1998**, 402–404, 32.
- (7) Memmel, N. *Surf. Sci. Rep.* **1998**, 32, 91.
- (8) Giergiel, J.; Kirschner, J.; Landgraf, J.; Shen, J.; Woltersdorf, J. *Surf. Sci.* **1994**, 310, 1.
- (9) Shen, J.; Klaua, M.; Ohresser, P.; Jenniches, H.; Barthel, J.; Mohan, Ch. V.; Kirschner, J. *Phys. Rev. B* **1997**, 56, 11134.
- (10) Jenniches, H.; Shen, J.; Mohan, Ch. V.; Manoharan, S. S.; Barthel, J.; Ohresser, P.; Klaua, M.; Kirschner, J. *Phys. Rev. B* **1999**, 59, 1196.
- (11) Ohresser, P.; Shen, J.; Barthel, J.; Zheng, M.; Mohan, Ch. V.; Klaua, M.; Kirschner, J. *Phys. Rev. B* **1999**, 59, 3696.
- (12) Klaua, M.; Shen, J.; Ohresser, P.; Jenniches, H.; Barthel, J.; Mohan, Ch. V.; Kirschner, J. *IEEE Trans. Magn.* **1998**, 34, 1216.
- (13) Shi, S. K.; Lee, H. I.; White, J. M. *Surf. Sci.* **1981**, 102, 56.
- (14) Shimizu, H.; Christmann, K.; Ertl, G. *J. Catal.* **1981**, 61, 412.
- (15) Hoffmann, F. M.; Paul, J. *J. Chem. Phys.* **1987**, 86, 2990.
- (16) Hoffmann, F. M.; Paul, J. *J. Chem. Phys.* **1987**, 87, 1857.
- (17) Willis, R. F. *Vibrational Spectroscopy of Adsorbates*; Springer-Verlag: Berlin, 1980.
- (18) Bell, A. T.; Hair, M. L. *Vibrational Spectroscopies for Adsorbed Species*; American Chemical Society: Washington, DC, 1980.
- (19) Hoffmann, F. M. *Surf. Sci. Rep.* **1983**, 3, 107.
- (20) Radnik, J.; Chopovskaya, E.; Grüne, M.; Wandelt, K. *Surf. Sci.* **1996**, 352–354, 268.
- (21) Grüne, M.; Radnik, J.; Wandelt, K. *Surf. Sci.* **1998**, 402–404, 236.
- (22) Egawa, C.; McCash, E. M. *J. Phys.: Condens. Matter* **1989**, 1, SB161.
- (23) Egawa, C.; Katayama, S.; Oki, S. *Appl. Surf. Sci.* **1997**, 121–122, 587.
- (24) Tanabe, T.; Suzuki, Y.; Wadayama, T.; Hatta, A. *Surf. Sci.* **1999**, 427–428, 414.
- (25) Tanabe, T.; Shibahara, T.; Buckmaster, R.; Ishibashi, T.; Wadayama, T.; Hatta, A. *Surf. Sci.* **2000**, 466, 1.
- (26) Tanabe, T.; Buckmaster, R.; Ishibashi, T.; Wadayama, T.; Hatta, A. *Surf. Sci.* **2001**, 472, 1.
- (27) Pritchard, J.; Catterick, T.; Gupta, R. K. *Surf. Sci.* **1975**, 53, 1.
- (28) Hayden, B. E.; Kretschmar, K.; Bradshaw, A. M. *Surf. Sci.* **1985**, 155, 553.
- (29) Horn, K.; Pritchard, J. *Surf. Sci.* **1976**, 55, 706.
- (30) Horn, K.; Hussain, M.; Pritchard, J. *Surf. Sci.* **1977**, 63, 244.
- (31) Benndorf, C.; Kruger, B.; Thieme, F. *Surf. Sci.* **1985**, 163, L675.
- (32) Bartosch, C. E.; Whitman, L. T.; Ho, W. *J. Chem. Phys.* **1986**, 85, 1052.
- (33) Erley, W. *J. Vac. Sci. Technol.* **1981**, 18, 472.
- (34) Tanabe, T.; Suzuki, Y.; Wadayama, T.; Hatta, A. *Surf. Sci.* **1996**, 352–354, 268.
- (35) Horn, K.; Pritchard, J. *Surf. Sci.* **1976**, 55, 701.
- (36) Ludviksson, A.; Ernst, K. H.; Zhang, R.; Campbell, C. T. *J. Catal.* **1993**, 141, 380.
- (37) Brodde, A.; Neddermeyer, H. *Surf. Sci.* **1993**, 278–288, 988.
- (38) Wuttig, M.; Feldmann, B.; Thomassen, J.; May, F.; Zillgen, H.; Brodde, A.; Hannemann, H.; Neddermeyer, H. *Surf. Sci.* **1993**, 291, 14.
- (39) Chambliss, D. D.; Johnson, K. E. *Surf. Sci.* **1994**, 313, 215.
- (40) Johnson, K. E.; Chambliss, D. D.; Wilson, R. J.; Chiang, S. *Surf. Sci.* **1994**, 313, L811.
- (41) Shen, J.; Schmidhals, C.; Woltersdorf, J.; Kirschner, J. *Surf. Sci.* **1998**, 407, 90.
- (42) Chambliss, D. D.; Wilson, R. J.; Chiang, S. *J. Vac. Sci. Technol., A* **1992**, 10, 1993.
- (43) Johnson, K. E.; Chambliss, D. D.; Wilson, R. J.; Chiang, S. *J. Vac. Sci. Technol., A* **1993**, 11, 1654.
- (44) Chambliss, D. D.; Johnson, K. E.; Wilson, R. J.; Chiang, S. *J. Magn. Mater.* **1993**, 121, 1.
- (45) Chambliss, D. D.; Johnson, K. E. *Phys. Rev. B* **1994**, 50, 5012.
- (46) Moskovits, M.; Hulse, J. E. *Surf. Sci.* **1976**, 61, 302.
- (47) Bagus, P. S.; Müller, W. *Chem. Phys. Lett.* **1985**, 115, 540.
- (48) Spišák, D.; Hafner, J. *Phys. Rev. B* **2001**, 64, 094418.
- (49) Chesters, M. A.; Pritchard, J. *Surf. Sci.* **1971**, 28, 460.
- (50) Kaua, M.; Höche, H.; Jenniches, H.; Barthel, J.; Kirschner, J. *Surf. Sci.* **1997**, 381, 106.
- (51) Kessler, K.; Thieme, F. *Surf. Sci.* **1977**, 67, 405.
- (52) Burton, J. J.; Jura, G. *J. Phys. Chem.* **1967**, 71, 1937.